Dentomaxillofacial Radiology (2022) 51, 20210314

birpublications.org/dmfr

RESEARCH ARTICLE

Exploring digital filters for internal root resorption: how can we improve the diagnosis of small lesions?

[1]Priscila Fernanda da Silveira Tiecher, [1]Nádia Assein Arús, [1,2]Eduarda Adams Hilgert, [1]Heloisa Emilia Dias da Silveira, [3]Mathias Pante Fontana, [1]Heraldo Luís Dias da Silveira and [1]Mariana Boessio Vizzotto

[1]Department of Surgery and Orthopedics, Oral Radiology Division, Federal University of Rio Grande do Sul, Porto Alegre, Brazil; [2]Postgraduate Program, Dental School, Federal University of Rio Grande do Sul, Porto Alegre, RS, Brazil; [3]Diagnostic Imaging Center in Dentistry (CDI), Porto Alegre, Brazil

Objectives: This study aimed to evaluate the impact of enhancement filters in detecting small simulated internal root resorptions (IRR).
Methods: : Forty-two extracted human teeth were sectioned, connected, and stored in a dry human jaw and X-rayed with photostimulable phosphor plates (PSPs), composing the control group (CG). In the middle-third of the root canals, IRR lesions were simulated using Da Silveira protocol. Later, the specimens were X-rayed to create the test group (TG). All images acquired were exported with seven enhancement filters plus the original image. Three examiners used a five-point Likert scale to evaluate the images regarding the presence/absence of IRR. Diagnostic efficacy was assessed from sensitivity and specificity results. Comparison among filters was performed by using receiver operating characteristic (ROC) curve analysis.
Results: : Moderate values of Kappa interexaminer (0.403–0.620) and high values of Kappa intraexaminer (0.757–0.915) were observed. The best performance occurred in the CG ($p < 0.05$). Original images presented the greatest sensitivity and area under the ROC curve (0.595–0.750), while the Endo filter presented the greatest specificity (0.952). Inversion and Pseudo-3D images produced the greatest doubt in the diagnosis, significant for CG with the Pseudo-3D filter ($p < 0.05$).
Conclusions: : The Original and 'Endo' filters should be chosen as it offers greater diagnostic ability and allows more confidence during the evaluation.
Dentomaxillofacial Radiology (2022) **51**, 20210314. doi: 10.1259/dmfr.20210314

Cite this article as: da Silveira Tiecher PF, Assein Arús N, Adams Hilgert E, Dias da Silveira HE, Pante Fontana M, Dias da Silveira HL, et al. Exploring digital filters for internal root resorption: how can we improve the diagnosis of small lesions?. *Dentomaxillofac Radiol* (2022) 10.1259/dmfr.20210314.

Keywords: root resorption; dental digital radiography; radiographic image enhancement

Introduction

The aetiology of internal root resorption (IRR) is related to pulpitis,[1] and the clinical sign of pain is rarely present.[2,3] I IRR is the result of dentin loss from the root canal due to the action of clastic cells[1,4,5] and, if untreated, progression of the lesion may result in premature loss of the tooth.[1,3] Early detection of small IRR lesions is essential to the viability of endodontic treatment[1,2,5] and higher treatment success rates.[1–3]

Periapical radiography is the first-choice examination for assessment of IRR lesions that may be detected as a radiographic finding,[6] which demands considerable attention from the professional when evaluating images.[3] The radiographic appearance includes the presence of an oval radiolucent area surrounding the root canal

Correspondence to: Mrs Mariana Boessio Vizzotto, E-mail: mariana.vizzotto@ufrgs.br;mari.vizzotto@gmail.com

Received 02 July 2021; revised 04 November 2021; accepted 07 November 2021; published online 23 November 2021

region.[1,3,4] In the event that presence of an IRR lesion is detected, radiographs should be taken from several different angles[1,2] because additional images can provide information regarding the location or type of lesion that is arising.[2] Digital radiographs offer some advantages over film-based systems, such as lower radiation doses and elimination of the need for chemical processing.[7,8] Enhancement filters have attracted research interest[9–13] because they enable the visual appearance of digital images to be improved. Notwithstanding, few studies have analyzed the capacity to diagnose IRR using these filters.[14–18] In general, studies that aim to compare the diagnostic capabilities of different imaging systems tend to use *in vitro* samples because of ethical principles and the need for radioprotection.[14–17] Such studies simulate IRR lesions using drills, following the Andreasen protocol.[19] However, despite the advantages of this standardization, drills generate cavities with different characteristics to clinical lesions[20] and can therefore influence interpretation of diagnostic tests as a consequence.

In response to this issue, a new IRR methodology for *in vitro* studies has been developed based on the use of acid demineralization[21] to generate artificial lesions that are more similar to physiological ones. In contrast with drill-created lesions, this methodology results in lesions closer to those found clinically, with irregular borders. Therefore, this study aimed to evaluate the diagnostic capability of digital radiography with digital filters for detecting small IRR lesions created using acid demineralization.

Methods and materials

The Research Ethics Committee at the Universidade Federal do Rio Grande do Sul (UFRGS) approved this study (No. 23378). The methodology used in the study is the same as in Da Silveira et. al.[21] Forty-two extracted canine and mandibular premolars were acquired from a human tooth bank Universidade Franciscana de Santa Maria - RS. The inclusion criteria were teeth with no restorations, endodontic treatment, signs of fissures or root fractures, and with pulp chambers and root canals free from any visible changes.

Development of small IRR lesions

The IRR lesions were produced adopting the same sequence and steps as used by Silveira et al[21] for small lesions. This protocol produces artificial IRR lesions of around 2 mm in diameter and 0.2 mm in depth, and is appropriate for the main objective of testing radiographic detection of minor lesions. Teeth were sectioned mesiodistally with a diamond disk (Buehler Diamond Cut-Off Wheels, No. 114243, Buehler, Lake Bluff, USA) using an electric cutter (IsoMet, Low-Speed Saw, Buehler, Lake Bluff, USA). The IRR was simulated using a protocol stipulating one day of acid demineralization at the middle third of the root canals. Lesions were created using 5% nitric acid for 12 h, 8% sodium hypochlorite for 10 min, and 5% nitric acid for 12 h. Residues were removed by immersion in deionized water for 24 h. Superimposition of the root sections followed this stage.

Image acquisition

The corresponding root sections were superimposed and inserted into alveoli produced in a dry human jaw, which was coated with a 5-mm wax layer to simulate soft tissue. A paralleling ring system was used to ensure parallelism between the tooth and the phosphor plate, with a distance of 30 cm from teeth to the X-ray emitter. The vertical angle was perpendicular to the buccal surface, and images were acquired in orthogonal (0°), mesial (15°) and distal (15°) views. Three image acquisitions were therefore executed for each tooth.

The control group (CG) consisted of all teeth radiographed before the IRR simulation (n = 42). Following simulation of the small IRR lesions, each tooth was radiographed again, and these comprised the test group (TG, n = 42) and the gold standard group (GS). The phosphor plate storage system (Vista Scan - Dürr Dental, Bietigheim-Bissingen, Germany) was used in the same X-ray equipment (Dabi Atlante, Spectre 70X, 127V, 8A, 50/60 Hz) with an exposure time of 0.4 s and 20 LP/mm (1000 dpi) spatial resolution. DBSWIN software (Dürr Dental AG, Bietigheim - Bissingen, Germany) was used to post-process the images using the Original (unfiltered) setting and Fine, Caries 1, Caries 2, Endo, Perio, Inversion and Pseudo-3-dimensional (3D) filters. Subsequently, the images were exported in Tagged Image File Format (TIFF). Figure 1 shows an example of the original image and the filters used for a tooth with an IRR lesion. An unblinded researcher (P.F.S.) determined the GS using the samples and their respective radiographic images.

Imaging evaluation

Eighty-four groups of radiographs taken at orthogonal, mesial and distal angles were arranged in coded groups. Each group was multiplied by the eight different versions of each image (seven filters and the unfiltered image), totaling 672 groups of images evaluated. A randomized and blinded sequence was prepared for the evaluations. Digital radiographs were viewed on a flat panel monitor (LG, Screen Size 21.5 inches, Contrast 30.000:1 DFC, Maximum Resolution 1920 × 1080), using the Windows® Image Viewer (Microsoft®) in a darkened room. The zoom tool was available. Three oral and maxillofacial radiologists analysed the images and 10% of the sample was reexamined to verify the intra-examiner agreement. Before starting the analysis, the observers were given instructions about the aims of the study and the scoring scale database. Evaluations were scored on a 5-point Likert scale, as follows: (1) conclusive presence of IRR; (2) probable presence of IRR; (3) uncertain presence of IRR; (4) probable absence of IRR; and (5) conclusive absence of IRR.

Data analysis

Statistical analysis was performed using SPSS software v. 22 (SPSS, Chicago, IL, USA), adopting a cutoff

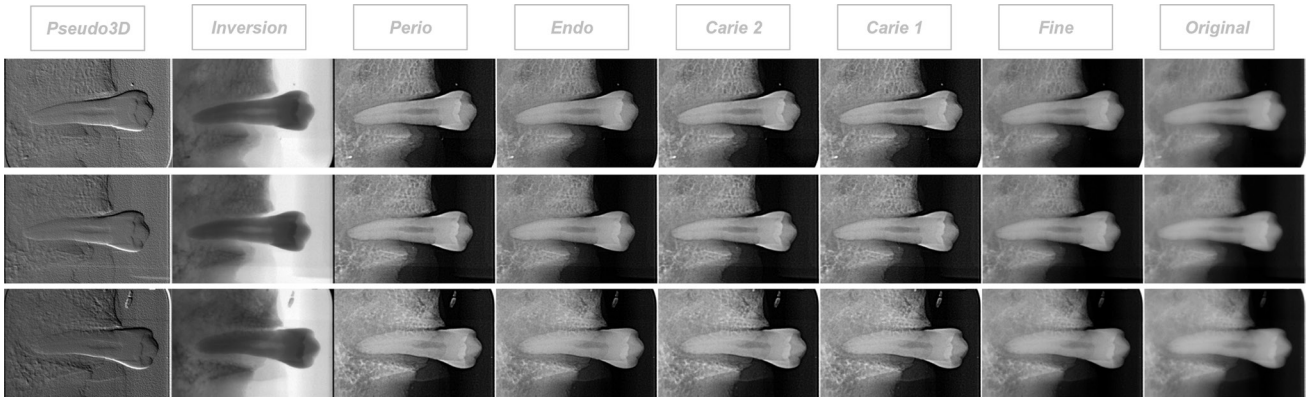

Figure 1 Radiographic images; original (unfiltered) and with post-processing filters, showing a tooth with IRR.

of $p \leq 0.05$. The κ index was used to analyze intra-examiner agreement and pairwise inter-examiner agreement. The mode of the three examiners' ratings was used for the sequence analyses. The accuracy for each filter in the CG and TG groups was verified. For this assessment, the responses scored on the 5-point Likert scale were dichotomized into the presence of IRR (scales 1 and 2) versus the absence of IRR (scales 3, 4 and 5). Sensitivity and specificity values and the area under the receiver operating characteristic (ROC) curve (auROC) were calculated with 95% confidence intervals (CI) for each filter using the generalized estimation equation (GEE). Diagnostic ability was analyzed using the 5-point Likert scale ratings by calculating the distance from the mean value attributed for each filter to the gold standard (GS). This was achieved by taking the mode of the three examiners' ratings and for each case, calculating the mean value of the modes for all cases per filter, and then measuring the distance from this value to the GS.

Results

The κ index (Table 1) showed that inter-examiner agreement was greatest between Ex1 and Ex3, and that the intra-examiner agreement ranged between 0.757 and 0.915. Table 2 shows that all of the filters achieved higher values for specificity than for sensitivity. It was also observed that the original images had higher values for sensitivity (0.595) and for auROC (0.750). There were no statistical differences between the filters when analyzed according to the auROC ($p = 0.533$). Comparing the CG to the TG, the percentages of correct diagnoses were significantly different ($p < 0.01$). The CG presented a higher percentage than TG; *that is,* specificity values were statistically higher than sensitivity values, regardless of the filter used.

Table 3 shows that the largest distances from the mode of the 5-point Likert scale scores to the GS were observed in the TG ($p < 0.05$). For the CG images, the 'Endo' filter exhibited the smallest distance (greatest diagnostic ability), while the largest distance was observed when applying the 'Pseudo3D' filter (smallest diagnostic ability). In the TG, the original image (unfiltered) and the 'Inversion' filter exhibited the shortest and largest distances from the GS, respectively. Table 3 also shows that, according to the Bonferroni test, there were no differences between the filters in the TG (the absence of filter resulted in greatest ability to diagnose IRR). In the CG, the diagnostic ability of the 'Endo', 'Caries 2', 'Perio' and 'Inversion' filters was statistically different to that of the 'Pseudo3D' filter.

Table 1 κ index results for analysis of intra-examiner and inter-examiner agreement

Inter Ex	*Ex1*	*Ex2*	*Ex3*
Ex3	0.620	0.403	
Ex1		0.547	0.620
Intra Ex	0.839	0.915	0.757
Gold-Std	0.397	0.591	0.357

Table 2 Sensitivity, specificity and auROC (CI = 95%) evaluating the means of mode scores for each post-processing filter

Filter	*Spec*	*Sen*	*auROC*	*CI 95%*
Original	0.905	0.595	0.750	(0.642; 0.857)
Fine	0.929	0.500	0.714	(0.602; 0.826)
Caries 1	0.929	0.500	0.714	(0.602; 0.826)
Caries 2	0.929	0.452	0.690	(0.575; 0.805)
Endo	0.952	0.500	0.726	(0.615; 0.836)
Perio	0.929	0.500	0.714	(0.602; 0.826)
Inversion	1.000	0.452	0.726	(0.615; 0.836)
Pseudo-3D	0.905	0.476	0.690	(0.575; 0.805)
**p = 0.377(>0.05)*	***p < 0.01*		****p = 0.533(>0.05)*	

Generalized equation estimation (GEE) model: *interaction factor between group and filter ($p = 0.377$); **difference within TG (sensitivity) e CG (specificity) ($p < 0.01$). ***difference between filters as a principal factor ($p = 0.533$); Spec = Specificity; Sen = Sensitivity; auROC = area under the ROC curve (receiver cooperating characteristics); CI = confidence interval.

Table 3 Mean distance from the mean of mode 5-point Likert scale scores for each filter to the gold-standard.

Group	*Filter*	*Mean distance*	*SDa*	*SE***	*BMC*
Without IRR (CG)	*Original*	0.381	0.91	0.139	AB
	Fine	0.333	0.90	0.138	AB
	Caries 1	0.333	0.90	0.138	AB
	Caries 2	0.262	0.83	0.126	B
	Endo	0.238	0.73	0.111	B
	Perio	0.286	0.83	0.127	B
	Inversion	0.310	0.47	0.071	B
	Pseudo3D	0.690	0.64	0.098	A
With IRR (TG)	*Original*	1.929	1.49	0.227	A
	Fine	2.071	1.64	0.251	A
	Caries 1	2.167	1.54	0.236	A
	Caries 2	2.095	1.56	0.238	A
	Endo	2.119	1.61	0.246	A
	Perio	2.071	1.60	0.244	A
	Inversion	2.238	1.25	0.190	A
	Pseudo3D	2.167	1.23	0.187	A

[a]SD = Standard Deviation; **EP = Standard Error; BMC = Bonferroni multiple comparison; Different uppercase letter indicates statistical difference ($p < 0.05$).

Discussion

It is essential to detect small IRR lesions to achieve successful endodontic treatment.[1–3,5] The function of the digital filters used in this study is to adjust the image parameters by removing undesirable information.[22] High-pass filters specifically make the 'edges' of the images more distinct.[23] The high-pass filters used in the study were 'Fine', 'Caries1', 'Caries2', 'Endo' and 'Perio'.[11] Three experienced examiners performed the evaluations and then the mean was calculated of the modes of their results for each case to reduce bias introduced by individual interpretations. κ index values for intra-examiner and inter-examiner agreement were moderate, similar to previous studies.[15,17] Intra-examiner agreement rates (0.757–0.915) were higher than inter-examiner agreement rates (0.403–0.620), suggesting that, in addition to the image filters, evaluators' perceptions could influence diagnoses.

Kamburoğlu et al, evaluated observers' ability to identify simulated IRR cavities using conventional film and digital images and concluded that the photostimulable phosphor method was less effective for detecting internal resorption. However, they pointed out that maybe the low-resolution system could influence the results.[24] In our study, regardless of the filter, specificity values (0.905 to 0.100) were higher ($p < 0.01$) than sensitivity values (0.452 to 0.595). The percentage of correct diagnoses was higher in the CG, suggesting that providers may have difficulty distinguishing small IRR lesions from normal morphological variants in root canals. The lower sensitivity values are possibly due to the methodology based on acid demineralization instead of lesions created by drilling, since the former are closer to those found clinically, with irregular limits. Previous studies evaluating small IRR lesions simulated using drills have found higher accuracy values. However, this may have occurred because of the well-outlined shape of the cavities, which perhaps makes identification easier.[15,16] The site of formation of IRR lesions directly influenced their detection, and some studies detected these differences,[17] while others did not.[16] The IRR was simulated in the middle third of the root, the most frequent site in clinical situations.[20] In general, the accuracy values found were similar between the different filters used. These findings support other studies that have evaluated diverse clinical conditions.[10,14]

Radiographs are usually the initial imaging exam used when investigating IRR because of the shorter time needed and lower cost and radiation dose. However, use of three-dimensional images is expanding, especially in Endodontics.[25] Studies that found low or moderate diagnostic accuracy values using 2D radiographs compared to CBCT explained these findings because of the difficulties involved in using 2D images, such as superimposition.[15,17,18] However, a study comparing micro-CT measurements of IRR cavities with those obtained by confocal laser scanning microscope concluded that micro-CT underestimated diameters and volumes.[26]

In this investigation, the original image presented a strong trend to superiority, even though statistical significance was not attained. This result corroborates other studies that recommend using these images to increase diagnostic ability.[9,11,22] It was observed that the inversion filter presented the highest mean accuracy in the CG, but that the same filter presented the lowest mean accuracy in the TG. These results may suggest that use of the Inversion filter introduces a high level of difficulty for evaluating IRR, causing examiners to diagnose IRR less accurately. A study from Nastaran Farhadi et al[27] reported low values of accuracy after evaluating the inversion filter for determining endodontic measurements. Furthermore, the inversion filter was not recommended for diagnosis of proximal caries.[10]

This study's findings point to the importance of professional knowledge, since digital images are usually available with some post-processing filters. Presence of radiopaque materials, such as restorations and prostheses, can cause image artefacts and reduce diagnostic accuracy when enhancement filters are used.[13] In this study, all teeth with restorations or prostheses were excluded, which may explain why some enhancement filters did not interfere with diagnosis.

The 5-point Likert scale provides a measure of the examiner's level of confidence in the diagnosis defined. It was observed that evaluations conducted with the 'Endo' filter resulted in more accurate diagnoses for absence of IRR than the other filters. However, the Pseudo-3D filter resulted in higher levels of doubt about absence of IRR. The greatest capability to diagnose IRR was obtained using the original image, while the

'Inversion' filter was associated with greatest doubt with relation to whether IRR lesions were present.

In conclusion, the Original unfiltered image or the 'Endo' filter should be chosen since they offer greater diagnostic ability and greater confidence during the evaluation. The inversion and Pseudo-3D filters should not be used for evaluation of small IRR because they increase doubt and probability of diagnostic error.

Acknowledgment

All authors affirm that they have no financial affiliation or involvement with any commercial organization with direct financial interest in the subject or materials discussed in this manuscript.

REFERENCES

1. Nilsson E, Bonte E, Bayet F, Lasfargues J-J. Management of internal root resorption on permanent teeth. *Int J Dent* 2013; **2013**: 1–7. doi: https://doi.org/10.1155/2013/929486
2. Darcey J, Qualtrough A. Resorption: Part 2. *Diagnosis and management. Br Dent J* 2013; **214**: 493–509.
3. Fernandes M, de Ataide I, Wagle R. Tooth resorption part I - pathogenesis and case series of internal resorption. *J Conserv Dent* 2013; **16**: 4–8. doi: https://doi.org/10.4103/0972-0707.105290
4. Patel S, Ricucci D, Durak C, Tay F. Internal root resorption: a review. *J Endod* 2010; **36**: 1107–21. doi: https://doi.org/10.1016/j.joen.2010.03.014
5. Consolaro A. The four mechanisms of dental resorption initiation. *Dental Press J Orthod* 2013; **18**: 7–9. doi: https://doi.org/10.1590/S2176-94512013000300004
6. Vasconcelos K de F, Rovaris K, Nascimento EHL, Oliveira ml, Távora D de M, Bóscolo FN. diagnostic accuracy of phosphor plate systems and conventional radiography in the detection of simulated internal root resorption. *Acta Odontol Scand* 2017; **75**: 573–6.
7. Wenzel A, Møystad A. Work flow with digital intraoral radiography: a systematic review. *Acta Odontol Scand* 2010; **68**: 106–14. doi: https://doi.org/10.3109/00016350903514426
8. de Oliveira ML. Pinto GC de S, Ambrosano GMB, Tosoni GM. Effect of combined digital imaging parameters on endodontic file measurements. *J Endod* 2012; **38**: 1404–7.
9. Leonardi RM, Giordano D, Maiorana F, Greco M. Accuracy of cephalometric landmarks on monitor-displayed radiographs with and without image emboss enhancement. *Eur J Orthod* 2010; **32**: 242–7. doi: https://doi.org/10.1093/ejo/cjp122
10. Belém MDF, Tabchoury CPM, Ferreira-Santos RI, Groppo FC, Haiter-Neto F. Performance of a photostimulable storage phosphor digital system with or without the sharpen filter and cone beam CT for detecting approximal enamel subsurface demineralization. *Dentomaxillofac Radiol* 2013; **42**: 20120313. doi: https://doi.org/10.1259/dmfr.20120313
11. de Azevedo Vaz SL, Neves FS, Figueirêdo EP, Haiter-Neto F, Campos PSF. Accuracy of enhancement filters in measuring in vitro peri-implant bone level. *Clin Oral Implants Res* 2013; **24**: 1074–7. doi: https://doi.org/10.1111/j.1600-0501.2012.02511.x
12. Nascimento HAR, Ramos ACA, Neves FS, de-Azevedo-Vaz SL, Freitas DQ. The 'Sharpen' filter improves the radiographic detection of vertical root fractures. *Int Endod J* 2015; **48**: 428–34. doi: https://doi.org/10.1111/iej.12331
13. Liedke GS, Spin-Neto R, Vizzotto MB, Da Silveira PF, Silveira HED, Wenzel A. Diagnostic accuracy of conventional and digital radiography for detecting misfit between the tooth and restoration in metal-restored teeth. *J Prosthet Dent* 2015; **113**: 39–47. doi: https://doi.org/10.1016/j.prosdent.2014.08.003
14. Kamburoğlu K, Kursun S. A comparison of the diagnostic accuracy of CBCT images of different voxel resolutions used to detect simulated small internal resorption cavities. *Int Endod J* 2010; **43**: 798–807. doi: https://doi.org/10.1111/j.1365-2591.2010.01749.x
15. Kamburoğlu K, Kurşun S, Yüksel S, Oztaş B. Observer ability to detect ex vivo simulated internal or external cervical root resorption. *J Endod* 2011; **37**: 168–75. doi: https://doi.org/10.1016/j.joen.2010.11.002
16. Stephanopoulos G, Mikrogeorgis G, Lyroudia K. Assessment of simulated internal resorption cavities using digital and digital subtraction radiography: a comparative study. *Dent Traumatol* 2011; **27**: 344–9. doi: https://doi.org/10.1111/j.1600-9657.2011.01020.x
17. Madani Z, Moudi E, Bijani A, Mahmoudi E. Diagnostic accuracy of cone-beam computed tomography and periapical radiography in internal root resorption. *Iran Endod J* 2016; **11**: 51–6. doi: https://doi.org/10.7508/iej.2016.01.010
18. Lima TF, Gamba TO, Zaia AA, Soares AJ. Evaluation of cone beam computed tomography and periapical radiography in the diagnosis of root resorption. *Aust Dent J* 2016; **61**: 425–31. doi: https://doi.org/10.1111/adj.12407
19. Andreasen FM, Sewerin I, Mandel U, Andreasen JO. Radiographic assessment of simulated root resorption cavities. *Endod Dent Traumatol* 1987; **3**: 21–7. doi: https://doi.org/10.1111/j.1600-9657.1987.tb00167.x
20. Gabor C, Tam E, Shen Y, Haapasalo M. Prevalence of internal inflammatory root resorption. *J Endod* 2012; **38**: 24–7. doi: https://doi.org/10.1016/j.joen.2011.10.007
21. da Silveira PF, Vizzotto MB, Montagner F, da Silveira HLD, da Silveira HED. Development of a new in vitro methodology to simulate internal root resorption. *J Endod* 2014; **40**: 211–6. doi: https://doi.org/10.1016/j.joen.2013.07.007
22. Brasil DM, Yamasaki MC, Santaella GM, Guido MCZ, Freitas DQ, Haiter-Neto F. Influence of VistaScan image enhancement filters on diagnosis of simulated periapical lesions on intraoral radiographs. *Dentomaxillofac Radiol* 2019; **48**: 20180146. doi: https://doi.org/10.1259/dmfr.20180146
23. Wenzel A, Haiter-Neto F, Frydenberg M, Kirkevang L-L. Variable-resolution cone-beam computerized tomography with enhancement filtration compared with intraoral photostimulable phosphor radiography in detection of transverse root fractures in an in vitro model. *Oral Surg Oral Med Oral Pathol Oral Radiol Endod* 2009; **108**: 939–45. doi: https://doi.org/10.1016/j.tripleo.2009.07.041
24. Kamburoğlu K, Barenboim SF, Kaffe I. Comparison of conventional film with different digital and digitally filtered images in the detection of simulated internal resorption cavities--an ex vivo study in human cadaver jaws. *Oral Surg Oral Med Oral Pathol Oral Radiol Endod* 2008; **105**: 790–7. doi: https://doi.org/10.1016/j.tripleo.2007.05.030
25. Venskutonis T, Daugela P, Strazdas M, Juodzbalys G. Accuracy of digital radiography and cone beam computed tomography on periapical radiolucency detection in endodontically treated teeth. *J Oral Maxillofac Res* 2014; **5**: e1: e1: . doi: https://doi.org/10.5037/jomr.2014.5201
26. Kamburoglu K, Barenboim SF, Aritürk T, Kaffe I. Quantitative measurements obtained by micro-computed tomography and confocal laser scanning microscopy. *Dentomaxillofac Radiol* 2008; **37**: 385–91. doi: https://doi.org/10.1259/dmfr/57348961
27. Farhadi N, Shokraneh A, Mehdizadeh M. Effect of contrast inversion enhancement on the accuracy of endodontic file length determination in digital radiography. *J Clin Diagn Res* 2015; **9**: ZC102–5. doi: https://doi.org/10.7860/JCDR/2015/11767.5988